Journal of Human Genetics (2014) 59, 484–487

www.nature.com/jhg

ORIGINAL ARTICLE

A new acro-osteolysis syndrome caused by duplications including *PTHLH*

Mary J Gray[1], Margriet van Kogelenberg[1], Rachel Beddow[2], Tim Morgan[1], Paul Wordsworth[3], Deborah J Shears[4], Stephen P Robertson[1] and Jane A Hurst[5]

Parathyroid hormone-like hormone (PTHLH, MIM 168470) is a humoral factor, structurally and functionally related to parathyroid hormone, which mediates multiple effects on chondrocyte, osteoblast and osteoclast function. Mutations and copy number imbalances of the *PTHLH* locus and in the gene encoding its receptor, *PTHR1*, result in a variety of skeletal dysplasias including brachydactyly type E, Eiken syndrome, Jansen metaphyseal chondrodysplasia and Blomstrand type chondrodysplasia. Here we describe three individuals with duplications of the *PTHLH* locus, including two who are mosaic for these imbalances, leading to a hitherto unrecognized syndrome characterized by acro-osteolysis, cortical irregularity of long bones and metadiaphyseal enchondromata.
Journal of Human Genetics (2014) **59,** 484–487; doi:10.1038/jhg.2014.58; published online 10 July 2014

INTRODUCTION

Parathyroid hormone-like hormone (PTHLH) is an important regulator of endochondral bone development. It is produced by perichondrial cells and growth plate chondrocytes during skeletal development, and is responsible for maintaining these cells in an undifferentiated proliferative state through a paracrine mechanism. This proliferative state is achieved through suppression of *RUNX2* with a feedback loop to Indian Hedgehog (IHH) expression, modulating the timing of differentiation of chondrocytes.[1]

Several skeletal dysplasias are caused by mutations in either *PTHLH* or the gene encoding its G-protein-coupled receptor, *PTHR1* (MIM 168468). These conditions include Jansen metaphyseal chondrodysplasia (MIM 156400), Eiken syndrome (MIM 600002) and lethal Blomstrand chondrodysplasia (BOCD, MIM 215045). Pathogenic genomic rearrangements, deletions and loss-of-function point mutations in *PTHLH* cause brachydactyly type E (BDE2, MIM 613382) with short stature and oligodontia.[2,3] A single case of an increase in *PTHLH* copy number has been described in a female with short stature, disproportionate short limbs, symmetrical metaphyseal expansions with enchondromatosis and brachydactyly.[4]

Here, three individuals with osteolysis and metaphyseal dysplasia, associated with duplication of *PTHLH*, are reported. Their phenotypes extend the phenotypic spectrum associated with copy number variations at this locus.

MATERIALS AND METHODS

Case one

Case one (Family A; Figures 1a, c–h) is a female born after a normal pregnancy to non-consanguineous parents. Her mother was phenotypically normal; her father is described as case two. In the first year of life, left tibial bowing prompted a skeletal survey that demonstrated multiple wormian bones within the lambdoid suture. At 3 years of age, bowing of the left radius had developed and metaphyseal flaring was seen radiologically, most notable distally. Her height was on the 3rd centile and she demonstrated no dysmorphism at this age. Her primary dentition erupted around this time. By 5 years of age the bowing of her left forearm had increased (Figure 1g) and an osteomy was performed, but non-union resulted. Her fingertips were noted to be clubbed in appearance with variable shortening of the distal phalanges. A diagnosis of Hajdu–Cheney syndrome (MIM 102500) was considered. By 10 years of age her left forearm bowing had progressed further, with multiple fractures occurring at the left wrist. Her right clavicle was noted to be eroded at the medial end and she had osteopenia. Her facial features began to coarsen, with her forehead appearing wide and prominent. Her head circumference was at the 97th centile. At 11 years of age, radiographs showed coxa valga with thinned cortices of the femoral necks, hypoplasia of the iliac bones inferiorly with lateral supra-acetabular constrictions. Her rib morphology was abnormal, with a narrow thorax and the posterior ends of the ribs sloping downwards anteriorly.

At 12 years of age a magnetic resonance imaging demonstrated basilar invagination, an Arnold–Chiari malformation and mild dilation of the central canal at the C7/T1 level. Severe headaches and hydrocephalus secondary to progressive basilar invagination evolved (Figure 1e), requiring surgical decompression at age 15. She had significant osteoporosis and bisphosphonates were administered. Her height was at the 50th centile but she had short neck, and a disproportionately short trunk, attributable to an evolving scoliosis (Figure 1f). Hand radiographs revealed progressive acro-osteolysis, especially of her thumbs and index fingers, slender metacarpals and shortening of the right 3rd metacarpal (Figure 1h). Her facial appearance had coarsened further. Serum calcium, phosphate, alkaline phosphatase, parathyroid hormone levels and urinary calcium excretion were all within normal limits.

[1]Department of Women's and Children's Health, Dunedin School of Medicine, University of Otago, Dunedin, New Zealand; [2]Cytogenetics Laboratory, Genetics Health Service New Zealand, Wellington Hospital, Wellington, New Zealand; [3]Nuffield Orthopaedic Centre, Department of Rheumatology, Oxford, UK; [4]Oxford Regional Genetics Service, The Churchill Hospital, Oxford, UK and [5]Department of Genetics, The Hospital for Sick Children, London, UK
Correspondence: Professor SP Robertson, Department of Women's and Children's Health, Dunedin School of Medicine, University of Otago, Dunedin 9054, New Zealand.
E-mail: stephen.robertson@otago.ac.nz
Received 29 March 2014; revised 14 June 2014; accepted 15 June 2014; published online 10 July 2014

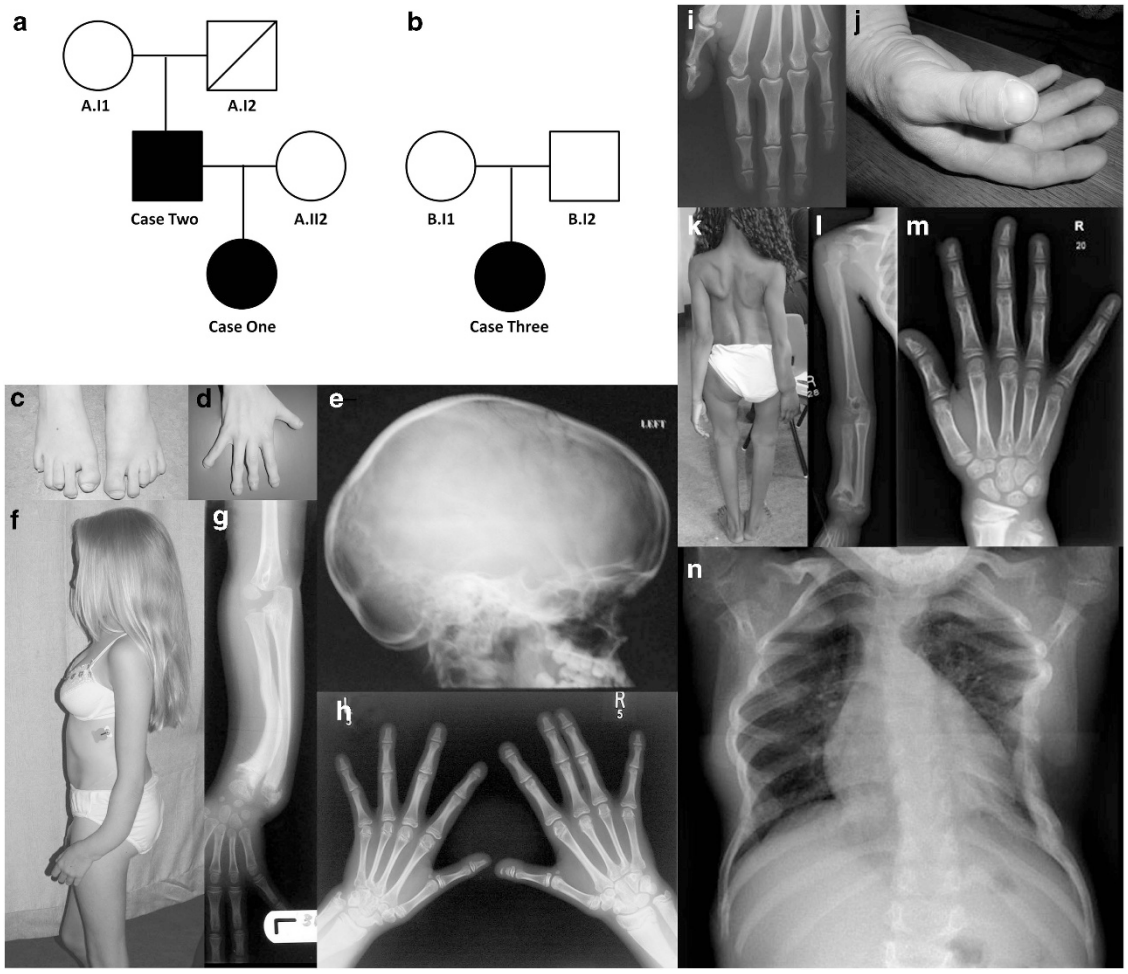

Figure 1 Clinical and radiographic presentation of the disorder in cases one–three. (**a**) Pedigree of family A, which includes cases one and two; (**b**) Pedigree of family B, which includes case three; (**c**–**h**) Case one demonstrating (**c**) clubbed great toes and (**d**) shortened distal phalanges especially evident in the thumb; (**e**) marked basilar invagination of the skull; (**f**) at age 12 years showing left forearm deformity; (**g**) metadiaphyseal irregularity in the ulna and radius with pronounced bowing; (**h**) acrosteolysis of terminal phalanges most evident in digits I and II; (**i**) Hand radiograph from case two; (**j**) distal phalangeal hypoplasia digit I in case two; (**k**–**n**) Case three demonstrating (**k**) asymmetric limb deformities, most pronounced in the right forearm; (**l**) radiolucencies affecting the proximal humerus, distal radius and ulna together with metadiaphyseal irregularity particularly of the radius; (**m**) mild distal phalangeal shortening especially digits 1 and II; (**n**) irregularity of rib length and form. A full color version of this figure is available at the *Journal of Human Genetics* journal online.

From the age of 12 to 18 years she developed asymmetry of the pelvis with rotation, and sustained fractures through the inferior pubic rami bilaterally that were managed conservatively. She developed increasing pain in both hips, initially worse on the right with substantial osteolysis of the acetabulum and femoral head that eventually resulted in avascular necrosis and a fractured acetabulum.

Case two

Case two (Family A; Figures 1a, i and j), the father of case one, had an unremarkable medical history. His parents had no abnormal skeletal manifestations. He was 170 cm tall, had no facial dysmorphism, a normal gait, and demonstrated no restriction in joint movements or propensity to fractures. The distal thumbs were short and spatulate in shape (Figures 1i and j).

Case three

Case three (Family B; Figures 1b and k–n) was the eldest of two children to healthy unrelated parents. The pregnancy and delivery were uncomplicated. She first walked at 11 months, shortly after which leg asymmetry was noted and bilateral radiolucencies were noted in the proximal femora. On evaluation at the of age 5 years her height was −3.6 s.d. and her occipito-frontal head circumference was 1.5 s.d. Her intellect was unimpaired. She had prominent eyes. Her teeth were normally erupted. She had one diffuse café-au-lait macule on the medial upper left arm. There was a positional scoliosis noted and upper limb deformities (Figure 1k). This was reflective of the presence of proximal femoral, radial and ulnar radiolucencies (Figure 1l), the latter being more severe on the right. These lesions were not painful but progressed to marked coxa valga. An osteotomy was performed at 9 years. At 11–12 years she had bilateral corrective osteotomies on the proximal femora. Excised tissue from the lesion consisted of irregular pieces of hyaline cartilage undergoing endochondral ossification to form lamellar trabecular bone. There were also adjacent areas of dense fibrous tissue with membranous bone formation. The trabecular bone showed fibrosis of the marrow spaces with no evidence of inflammation. Additional skeletal findings included thoracic hypoplasia with rib length irregularity (Figure 1n) and mild acro-osteolysis of the distal phalanges of digits I and II (Figure 1m). Plasma calcium, phosphate and parathyroid hormone were all normal. The urine calcium and urine calcium/creatinine ratios were normal. The urinary N-terminal telopeptide of type-I collagen/creatinine ratio was 2152 nmol mmol^{-1}, indicative of very high bone turnover.

PTHLH and *NOTCH2* exon 34[5] were amplified by PCR from genomic DNA. Genotyping for case one was performed on the Affymetrix Genome-Wide

Human SNP Array 6.0 platform. Analysis was performed within Affymetrix Genotyping Console and Partek Genomics Suite. Copy number variations with a probability score of $<1\times10^{-5}$ were checked against the Database of Genomic Variants (http://projects.tcag.ca/variation/) to exclude any common copy number variations. Array Comparative genomic hybridization was performed for case three on the NimbleGen 135 K v3.1 array. The Agilent ISCA 8×60 K v2 array was used to array comparative genomic hybridization for cases two and three. A multiplex ligation-dependent probe amplification probe set, consisting of 14 probes was designed, validated according to manufactures guidelines[6] (MRC-Holland, Amsterdam, The Netherlands). Probe sequences are available upon request. The threshold of the probe ratio denoting the presence of a deletion was set at $\leqslant0.70$ and for a duplication $\geqslant1.30$. Microsatellite *D12S1337* was amplified using low cycle number (26 cycles) PCR using fluorescently labeled primers, and alleles were resolved on an Applied Biosystems 3730xl DNA Analyser (Applied Biosystems, Foster City, CA, USA). The genotype files were analyzed in Gene Mapper V4.0 (Applied Biosystems). Three unrelated individuals with the three alleles of interest were control samples. This research was carried out under ethical approval granted by the New Zealand Multiregion Ethical committee (MEC 08/08/094).

RESULTS

Owing to the presence of osteopenia and acrosteolysis a diagnosis of Hajdu–Cheney syndrome (MIM 102500) was considered in case one and a DNA sample was screened for mutations in exon 34 of *NOTCH2*. No mutations were identified.

Affymetrix 6.0 Microarray data, processed through Partek Genomics Suite, on case one demonstrated a 0.85 Mb duplication on chromosome 12p11.22–p11.23 (chr12: 27 604 157–28 455 192, hg18) with an increase in copy number over 585 markers affecting six annotated genes, *PPFIBP1, REP15, MRPS35, KLHDC, PTHLH* and *CCDC91* (Figure 2). Genomic qPCR analysis confirmed that the telomeric breakpoint of the duplication occurred centromeric to exon 1 of *PPFIB1* and the centromeric breakpoint lay within intron 7 of *CCDC91*. Microduplications and deletions have been reported in this region in healthy controls in Database of Genomic Variants, but none encompassed the duplication detected in case one. Multiplex ligation-dependent probe amplification analysis corroborated the presence of the microduplication in case one and demonstrated that case two, the father of case one, was mosaic for the same duplication.

Copy number variation analysis, using the NimbleGen 135 K v3.1 array, on case three demonstrated the presence of a *de novo* copy number gain over a smaller (0.5 Mb) overlapping region of chromosome 12 (chr12: 27 615 800–28 118 440, hg18). Multiplex ligation-dependent probe amplification analysis on DNA extracted from saliva and blood leukocytes confirmed the presence and extent of this duplication, and also demonstrated that it was present in a mosaic state (Figure 2 and Supplementary Table S1). Both cases two and three were independently arrayed on the Agilent ISCA(v2) 8×60 K CGH array to further verify their mosaicism. Analysis of case three indicated a mosaic result. While the duplication was confirmed in case two, the array was unable to confirm the mosaicism (Supplementary Figure S1).

To determine the parental derivation of these duplications, the segregation and peak intensity of alleles of the dinucleotide repeat *D12S1337* were determined (Figure 2, Supplementary Figure S2 and Supplementary Table S2). This microsatellite maps within the *PTHLH* locus. In family A, the segregation of the 246 bp allele confirmed that the duplication arose *de novo* in case two on his maternally derived (A.I1) allele. Although case one is monoallelic for *D12S1337*, the segregation of alleles at this locus confirms case one has inherited the duplicated allele from her father. *PTHLH* was sequenced in both cases one and two, but no sequence variations were

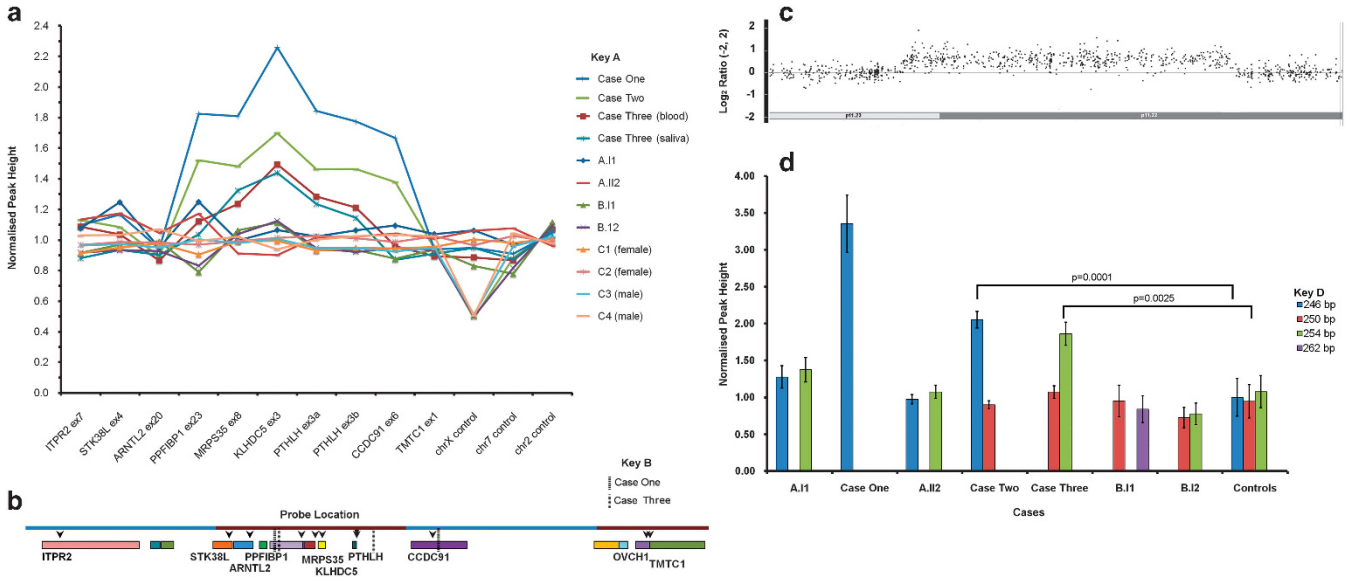

Figure 2 Duplications of *PTHLH* and neighboring genes in cases one–three. (**a**) Multiplex ligation-dependent probe amplification (MLPA) analysis of affected and unaffected individuals from families A and B together with four unrelated controls. DNA was sourced from blood leukocytes for cases one and two, and both blood and saliva for case three. Probe positions are as indicated in **b**. Diminished peak heights for cases two and three relative to case one are indicative of the mosaic status of their duplications; (**b**) diagram demonstrating gene content of the region duplicated in both families. Arrowheads indicate the position of MLPA probes. Dashed lines indicate the extent of the described duplications in families A and B. Bars indicate 1 Mb. (**c**) Array comparative genomic hybridization of case one demonstrating a duplication on Ch12p12.1–p11.22. (**d**) Semiquantitative *D12S1337* microsatellite analysis indicating elevated peak heights compared to controls for alleles located within *PTHLH* duplications. Peak heights are lower for individuals that are mosaic for the duplications. Replicates ($n=5$–16) refer to assays measured from independently performed PCRs; *P*-values are calculated using Student's *t*-test; error bars indicate s.e.m.

identified. In family B, case three's duplicated allele (254 bp) is derived from her father B.I2.

DISCUSSION

The condition described here is characterized by autosomal dominant metadiaphyseal abnormalities, including lesions radiographically resembling enchondromata, bowed long bones, acro-osteolysis, progressive osteoporosis and abnormal rib angulation.

Cases one and three are equal in phenotypic severity, despite the mosaicism in case three, while case two is skeletally eumorphic. It is possible that the degree of mosaicism of the duplicated allele is much higher in the skeleton than in blood leukocytes in case three, and therefore has resulted in a severe phenotype. Alternatively, the variation in phenotypes could be due to variable expressivity, where a mosaic case may present as clinically normal through to a phenotype as severe as an individual with a germline duplication.

The phenotype exhibits substantial clinical overlap with Hajdu–Cheney syndrome but with discriminating characteristics such as metadiaphyseal enchondromata of the long bones and rib malformations, as seen in Jansen metaphyseal chondrodysplasia, albeit to a milder degree.[7,8] The clinical similarities to Jansen metaphyseal chondrodysplasia, together with the involvement of *PTHLH* in both duplications, suggest that this disorder is related to the several entities already linked to mutations or genomic rearrangements at this locus.

The genetic evidence to support the duplication of *PTHLH* as the primary determinant of this phenotype is strong but not absolute. In case one, in addition to *PTHLH*, five additional genes are partially or wholly duplicated (*PPFIBP1, REP15, MRPS35, KLHDC5* and *CCDC91*) and in case three, only four (*PPFIBP1, REP15, MRPS35, KLHDC*). Of these genes, *PPFIBP1*, *MRPS35* and *CCDC91* have been documented to be duplicated without phenotypic effect in the Database of Genomic Variants. Of the two other genes, *KLHDC5* may regulate microtubular structure and interacts with the E3 ubiquitin ligase CUL3,[9] while *REP15* is a regulator of transferrin endocytosis.[10] Although the contribution of these two genes to the genesis of this phenotype cannot be excluded, the phenotypic similarity with other conditions characterized by overactivity of the PTHLH/PTHR1 axis suggests that microduplication of *PTHLH* is central to the pathogenesis of this skeletal dysplasia.[3,4] It could be inferred from these data that these duplications amplify *PTHLH* expression but this cannot be directly addressed in this study with the materials available, as *PTHLH* is neither expressed sufficiently in blood leukocytes or skin fibroblasts, nor is its protein product detectable in plasma under physiological conditions.

CONFLICT OF INTEREST

The authors declare no conflict of interest.

ACKNOWLEDGEMENTS

This work was supported by Curekids New Zealand.

1 Kronenberg, H. M. PTHrP and skeletal development. *Ann. NY Acad. Sci.* **1068,** 1–13 (2006).
2 Maass, P. G., Wirth, J., Aydin, A., Rump, A., Stricker, S., Tinschert, S. *et al.* A cis-regulatory site downregulates PTHLH in translocation t(8;12)(q13;p11.2) and leads to Brachydactyly Type E. *Hum. Mol. Genet.* **19,** 848–860 (2010).
3 Klopocki, E., Hennig, B. P., Dathe, K., Koll, R., de Ravel, T., Baten, E. *et al.* Deletion and point mutations of PTHLH cause brachydactyly type E. *Am. J. Hum. Genet.* **86,** 434–439.
4 Collinson, M., Leonard, S. J., Charlton, J., Crolla, J. A., Silve, C., Hall, C. M. *et al.* Symmetrical enchondromatosis is associated with duplication of 12p11.23 to 12p11.22 including PTHLH. *Am. J. Med. Genet. A* **152A,** 3124–3128.
5 Simpson, M. A., Irving, M. D., Asilmaz, E., Gray, M. J., Dafou, D., Elmslie, F. V. *et al.* Mutations in NOTCH2 cause Hajdu-Cheney syndrome, a disorder of severe and progressive bone loss. *Nat. Genet.* **43,** 303–305 (2011).
6 Eijk-Van Os, P. G. & Schouten, J. P. Multiplex ligation-dependent probe amplification (MLPA(R)) for the detection of copy number variation in genomic sequences. *Methods Mol. Biol.* **688,** 97–126.
7 Charrow, J. & Poznanski, A. K. The Jansen type of metaphyseal chondrodysplasia: confirmation of dominant inheritance and review of radiographic manifestations in the newborn and adult. *Am. J. Med. Genet.* **18,** 321–327 (1984).
8 Kozlowski, K., Campbell, J. B., Azouz, M. E. & Sprague, P. Metaphyseal chondrodysplasia, type Jansen. *Australas. Radiol.* **43,** 544–547 (1999).
9 Cummings, C. M., Bentley, C. A., Perdue, S. A., Baas, P. W. & Singer, J. D. The Cul3/Klhdc5 E3 ligase regulates p60/katanin and is required for normal mitosis in mammalian cells. *J. Biol. Chem.* **284,** 11663–11675 (2009).
10 Strick, D. J. & Elferink, L. A. Rab15 effector protein: a novel protein for receptor recycling from the endocytic recycling compartment. *Mol. Biol. Cell.* **16,** 5699–5709 (2005).

Supplementary Information accompanies the paper on Journal of Human Genetics website (http://www.nature.com/jhg)